



IMPLEMENTING MULTI-SCALE AGRICULTURAL INDICATORS EXPLOITING SENTINELS

**VEGETATION FIELD DATA AND PRODUCTION OF
GROUND-BASED MAPS:**

**“LA REINA SITE, CÓRDOBA, SPAIN”
19TH - 20TH MAY 2014**

ISSUE I1.10

EC Proposal Reference N° FP7-311766

Actual submission date : October 2014

Start date of project: 01.11.2012

Duration : 40 months

Name of lead partner for this deliverable: EOLAB



Book Captain: Consuelo Latorre (EOLAB)

Contributing Authors: Fernando Camacho (EOLAB)

M. Pat González, F.L. Muñoz (IFAPA)

Project co-funded by the European Commission within the Seventh Framework Program (2007-2013)		
Dissemination Level		
PU	Public	X
PP	Restricted to other programme participants (including the Commission Services)	
RE	Restricted to a group specified by the consortium (including the Commission Services)	
CO	Confidential, only for members of the consortium (including the Commission Services)	

DOCUMENT RELEASE SHEET

Book Captain:	C. Latorre	Date: 09.06.2016	Sign. 
Approval:	R. Lacaze	Date: 10.06.2016	Sign. 
Endorsement:	M. Koleva	Date:	Sign.
Distribution:	Public		

CHANGE RECORD

Issue/Revision	Date	Page(s)	Description of Change	Release
I1.00	01.10.2014	All	First Issue	I1.00
I1.10	09.06.2016	All	Included subsite	I1.10

TABLE OF CONTENTS

1.	<i>Background of the Document</i>	10
1.1.	Executive Summary	10
1.2.	Portfolio	10
1.3.	Scope and Objectives	11
1.4.	Content of the Document	11
2.	<i>Introduction</i>	12
3.	<i>Study area</i>	13
3.1.	Location	13
3.2.	Description of The Test Site	14
4.	<i>Ground measurements</i>	16
4.1.	Material and Methods	16
4.2.	Spatial Sampling Scheme	19
4.3.	ground data	20
4.3.1.	Data processing	20
4.3.2.	Content of the Ground Dataset	22
5.	<i>Evaluation of the sampling</i>	25
5.1.	Evaluation Based On Convex Hull: Product Quality Flag	25
6.	<i>production of ground-based maps</i>	27
6.1.	Imagery	27
6.2.	The Transfer Function	27
6.2.1.	The regression method	27
6.2.2.	Band combination	28
6.2.3.	The selected Transfer Function	29
6.3.	The High Resolution Ground Based Maps	30
6.3.1.	Mean Values	32
7.	<i>Conclusions</i>	34
8.	<i>Acknowledgements</i>	35
9.	<i>References</i>	36

LIST OF FIGURES

<i>Figure 1: Location of La Reina site in Córdoba, Spain.</i>	<i>13</i>
<i>Figure 2: False color composition of TOA Reflectance Landsat-8 image over the 5x5 km² study area (20th, May 2014) Left: Subsite 1. Right: Subsite 2.</i>	<i>13</i>
<i>Figure 3: Distribution of the fields over the study area. La Reina site, Córdoba (Spain).</i>	<i>14</i>
<i>Figure 4: Examples of the different land cover types in La Reina site – Córdoba (Spain). a) Chickpea, b) Onion, c) Sunflower, d) Wheat and e) Olive Tree.</i>	<i>15</i>
<i>Figure 5: Distribution of the sampling units (ESU) over the study area. DHP sampling and study zone of 5x5 km², over La Reina site, Córdoba (Spain).</i>	<i>19</i>
<i>Figure 6: Digital Hemispherical Photographs acquired in La Reina site, Córdoba (Spain) during the intensive campaign of 19-20 May 2014.</i>	<i>20</i>
<i>Figure 7: Intercomparison of the calculated biophysical variables LAI and LAI_{eff} over the ESUs with different methods: CEV5.1, CEV6.1 and Miller’s formula. La Reina site – Córdoba (Spain) during the campaign of 20th May, 2014.</i>	<i>20</i>
<i>Figure 8: Intercomparison of the measured biophysical variables over the ESUs, Effective LAI and LAI versus FAPAR. La Reina site – Córdoba (Spain) during the campaign of 20th May, 2014.</i>	<i>21</i>
<i>Figure 9: Results of the CAN-EYE processing carried out on cultivate area (ESU 19, Onion). (a) DHP images. (b, c) Classified images. (d) Average gap fraction and (e) the clumping factor versus view zenith angle.</i>	<i>21</i>
<i>Figure 10: LAI_{eff} measurements acquired in La Reina site – Córdoba, during the campaign of May 2014. Distribution by ESUs. (AS: Asparagus, C: Cotton, OT: Olive Tree plantation, SF: Sunflower, ON: Onion, CP: Chickpea, P: Potato, W: Wheat and BS: Bare Soil)</i>	<i>23</i>
<i>Figure 11: LAI measurements acquired in La Reina site – Córdoba, during the campaign of May 2014. As in figure 10 for LAI.</i>	<i>23</i>
<i>Figure 12: FAPAR instantaneous at 10:00h and FAPAR daily integrated measurements acquired in La Reina site – Córdoba, during the campaign of May 2014. As in figure 10 for FAPAR.</i>	<i>23</i>
<i>Figure 13: FCOVER measurements acquired in La Reina site – Córdoba, during the campaign of May 2014. As in figure 10 for FCOVER.</i>	<i>24</i>
<i>Figure 14: Distribution of the measured biophysical variables over the ESUs. La Reina site- Córdoba, during the campaign of 20th May, 2014.</i>	<i>24</i>
<i>Figure 15: Convex Hull test over 20x20 km² (Left) extended area centered at the test site and the 5x5 km² study area (Right top: Subsite 1, Right bottom: Subsite 2). Clear and dark blue correspond to the pixels belonging to the ‘strict’ and ‘large’ convex hulls. Red corresponds to the pixels for which the transfer function is extrapolating, La Reina –Córdoba (20th May 2014).</i>	<i>26</i>
<i>Figure 16: Test of multiple regression (TF) applied on different band combinations. Band combinations are given in abscissa (1=G, 2=RED, 3=NIR and 4=SWIR). The weighted root mean square error (RMSE) is presented in red along with the cross-validation RMSE in green. The numbers indicate the number of data used for the robust regression with a weight lower than 0.7 that could be considered as outliers.</i>	<i>28</i>
<i>Figure 17: LAI_{eff}, LAI, FAPAR and FCOVER results for regression on reflectance using 4 bands combination. Full dots: Weight>0.7. Empty dots: 0<Weight<0.7 crosses.</i>	<i>29</i>
<i>Figure 18: Ground-based LAI maps (20x20 km²) retrieved on the La Reina- Córdoba site (Spain). Left: LAI_{eff}. Right: LAI. (20th May 2014).</i>	<i>30</i>

<i>Figure 19: Ground-based FAPAR maps (20x20 km²) retrieved on the La Reina- Córdoba site (Spain). Top: Instantaneous FAPAR at 10:00 a.m. (20th May 2014).</i>	30
<i>Figure 20: Ground-based FCOVER map (20x20 km²) retrieved on the La Reina- Córdoba site (Spain). (20th May 2014).</i>	31
<i>Figure 21: Ground-based maps (5x5 km²) retrieved on the La Reina- Córdoba site (Spain) subsite 1. (20th May 2014).</i>	31
<i>Figure 22: Ground-based maps (5x5 km²) retrieved on the La Reina- Córdoba site (Spain) subsite 2. (20th May 2014).</i>	32

LIST OF TABLES

<i>Table 1: Coordinates and altitude of the test site (centre).....</i>	<i>14</i>
<i>Table 2: Summary of the field measurements in La Reina site – Córdoba (Spain).</i>	<i>19</i>
<i>Table 3: The Header used to describe ESUs with the ground measurements.</i>	<i>22</i>
<i>Table 4: Acquisition geometry of Landsat-8 data used for retrieving high resolution maps.</i>	<i>27</i>
<i>Table 5: Transfer function applied to the whole site for LA_{eff}, LAI, instantaneous FAPAR at 10:00 a.m. and FCOVER. RW for weighted RMSE, and RC for cross-validation RMSE.</i>	<i>29</i>
<i>Table 6: Mean values and standard deviation (STD) of the HR biophysical maps for the selected 3 x 3 km² area at La Reina site – Córdoba (Spain).....</i>	<i>32</i>

LIST OF ACRONYMS

CCD	Charge coupled devices
CEOS	Committee on Earth Observation Satellite
CEOS LPV	Land Product Validation Subgroup
DG AGRI	Directorate General for Agriculture and Rural Development
DG RELEX	Directorate General for External Relations (European Commission)
DHP	Digital Hemispheric Photographs
ECV	Essential Climate Variables
EUROSTATS	Directorate General of the European Commission
ESU	Elementary Sample Unit
FAPAR	Fraction of Absorbed Photo-synthetically Active Radiation
FAO	Food and Agriculture Organization
FCOVER	Fraction of Vegetation Cover
GCOS	Global Climate Observing System
GEO-GLAM	Global Agricultural Geo- Monitoring Initiative
GIO-GL	GMES Initial Operations - Global Land (GMES)
GCOS	Global Climate Observing System
GMES	Global Monitoring for Environment and Security
GPS	Global Positioning System
IMAGINES	Implementing Multi-scale Agricultural Indicators Exploiting Sentinels
IFAPA	Instituto de Investigación y Formación Agraria y Pesquera. Andalucía.
JECAM	Joint Experiment for Crop Assessment and Monitoring
LAI	Leaf Area Index
LDAS	Land Data Assimilation System
LUT	Look-up-table techniques
PAI	Plant Area Index
PROBA-V	Project for On-Board Autonomy satellite, the V standing for vegetation.
RMSE	Root Mean Square Error
SPOT /VGT	Satellite Pour l'Observation de la Terre / VEGETATION
SCI	GMES Services Coordinated Interface
TOA	Top of Atmosphere Reflectance
USGS	U.S. Geological Survey. Science organization.
UNFCCC	United Nations Framework Convention on Climate Change
UTM	Universal Transverse Mercator coordinates system
VALERI	Validation of Land European Remote sensing Instruments
WGCV	Working Group on Calibration and Validation (CEOS)
WGS-84	World Geodetic System

1. BACKGROUND OF THE DOCUMENT

1.1. EXECUTIVE SUMMARY

The Copernicus Land Service has been built in the framework of the FP7 geoland2 project, which has set up pre-operational infrastructures. ImagineS intends to ensure the continuity of the innovation and development activities of geoland2 to support the operations of the global land component of the GMES Initial Operation (GIO) phase. In particular, the use of the future Sentinel data in an operational context will be prepared. Moreover, IMAGINES will favor the emergence of new downstream activities dedicated to the monitoring of crop and fodder production.

The main objectives of ImagineS are to (i) improve the retrieval of basic biophysical variables, mainly LAI, FAPAR and the surface albedo, identified as Terrestrial Essential Climate Variables, by merging the information coming from different sensors (PROBA-V and Landsat-8) in view to prepare the use of Sentinel missions data; (ii) develop qualified software able to process multi-sensor data at the global scale on a fully automatic basis; (iii) complement and contribute to the existing or future agricultural services by providing new data streams relying upon an original method to assess the above-ground biomass, based on the assimilation of satellite products in a Land Data Assimilation System (LDAS) in order to monitor the crop/fodder biomass production together with the carbon and water fluxes; (iv) demonstrate the added value of this contribution for a community of users acting at global, European, national, and regional scales.

Further, ImagineS will serve the growing needs of international (e.g. FAO and NGOs), European (e.g. DG AGRI, EUROSTATS, DG RELEX), and national users (e.g. national services in agro-meteorology, ministries, group of producers, traders) on accurate and reliable information for the implementation of the EU Common Agricultural Policy, of the food security policy, for early warning systems, and trading issues. ImagineS will also contribute to the Global Agricultural Geo-Monitoring Initiative (GEO-GLAM) by its original agriculture service which can monitor crop and fodder production together with the carbon and water fluxes and can provide drought indicators, and through links with JECAM (Joint Experiment for Crop Assessment and Monitoring).

1.2. PORTFOLIO

The ImagineS portfolio contains global and regional biophysical variables derived from multi-sensor satellite data, at different spatial resolutions, together with agricultural indicators, including the above-ground biomass, the carbon and water fluxes, and drought indices resulting from the assimilation of the biophysical variables in the Land Data Assimilation System (LDAS).

The production in Near Real Time of the 333m resolution products, at a frequency of 10 days, using PROBA-V data is carried out in the Copernicus Global Land Service (<http://land.copernicus.eu/global/>).

The demonstration of high resolution (30m) products derived from Landsat-8 was done over demonstration sites of cropland and grassland in contrasting climatic and environmental conditions. Demonstration products are available on the ImagineS website (<http://www.fp7-imagines.eu/pages/services-and-products/landsat-8-biophysical-products.php>)

1.3. SCOPE AND OBJECTIVES

The main objective of this document is to describe the field campaign and ground data collected at La Reina site in Córdoba - Spain and the up-scaling of the ground data to produce ground-based high resolution maps of the following biophysical variable:

- Leaf Area Index (LAI), defined as half of the total developed area of leaves per unit ground surface area (m^2/m^2). We focused on two different LAI quantities (for green elements):
 - An effective LAI (LAI_{eff}) derived from the description of the gap fraction as a function of the view zenith angle. In addition, effective LAI measures derived at 57.5° are also provided in the ground database.
 - An actual LAI (LAI) estimate corrected from the clumping index.
- Fraction of green Vegetation Cover (FCover), defined as the proportion of soil covered by vegetation, derived from the gap fraction between 0 and 10° of view zenith angle.
- Fraction of Absorbed Photosynthetically Active Radiation (FAPAR), which is the fraction of the photosynthetically active radiation (PAR) absorbed by a vegetation canopy. PAR is the solar radiation reaching the canopy in the $0.4-0.7 \mu m$ wavelength region. We focused on the instantaneous 'black-sky' FAPAR at 10:00h SLT, which is the FAPAR under direct illumination conditions at a given solar position. In addition, two other quantities are provided in the ground database: daily integrated FAPAR computed as the black-sky FAPAR integrated over the day and the 'white-sky' FAPAR, which is the FAPAR under diffuse illumination conditions.

1.4. CONTENT OF THE DOCUMENT

This document is structured as follows:

- Chapter 2 provides an introduction to the field experiment.
- Chapter 3 provides the location and description of the site.
- Chapter 4 describes the ground measurements, including material and methods, sampling and data processing.
- Chapter 5 provides an evaluation of the sampling.
- Chapter 6 describes the production of high resolution ground-based maps, and the selected "mean" values for validation.

2. INTRODUCTION

Validation of remote sensing products is mandatory to guaranty that the satellite products meets the user's requirements. Protocols for validation of global LAIeff products are already developed in the context of Land Product Validation (LPV) group of the Committee on Earth Observation Satellite (CEOS) for the validation of satellite-derived land products (Fernandes et al., 2014), and recently applied to Copernicus global land products based on SPOT/VGT observation (Camacho et al., 2013). This generic approach is made of 2 major components:

- The indirect validation: including inter-comparison between products as well as evaluation of their temporal and spatial consistency
- The direct validation: comparing satellite products to ground measurements of the corresponding biophysical variables. In the case of low and medium resolution sensors, the main difficulty relies on scaling local ground measurements to the extent corresponding to pixels size. However, the direct validation is limited by the small number of sites, for that reason a main objective of ImagineS is the collection of ground truth data in demonstration sites.

The content of this document is compliant with existing validation guidelines (for direct validation) as proposed by the CEOS LPV group (Morissette et al., 2006); the VALERI project (<http://w3.avignon.inra.fr/valeri/>) and ESA campaigns (Baret and Fernandes, 2012). It therefore follows the general strategy based on a bottom up approach: it starts from the scale of the individual measurements that are aggregated over an elementary sampling unit (ESU) corresponding to a support area consistent with that of the high resolution imagery used for the up-scaling of ground data. Several ESUs are sampled over the site. Radiometric values over a decametric image are also extracted over the ESUs. This will be later used to develop empirical transfer functions for up-scaling the ESU ground measurements (e.g. Martínez et al., 2009). Finally, the high resolution ground based map will be compared with the medium resolution satellite product at the spatial support of the product.

An intensive field campaign to characterize the vegetation biophysical parameters at the La Reina (Córdoba) test site was carried out by EOLAB in collaboration with the IFAPA – *Instituto de Investigación y Formación Agraria y Pesquera*.

Intensive Field Campaign: 19th -20th of May 2014.

Teams involved in field collection:

EOLAB: F. Camacho, C. Latorre

Contact:

EOLAB: Fernando Camacho (fernando.camacho@eolab.es)

IFAPA: M. Pat González (mariap.gonzalez.d@juntadeandalucia.es)

3. STUDY AREA

3.1. LOCATION

“La Reina” site near Córdoba city belongs to the Córdoba Region, in Andalusia, southern Spain ($37^{\circ} 49' 26.7096''$ N, $4^{\circ} 52' 9.2886''$ W) (Figure 1 and Figure 2). The city is located on the banks of the Guadalquivir river.

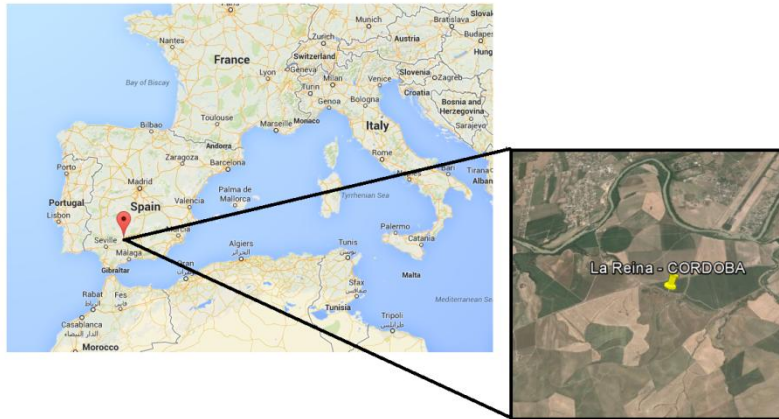


Figure 1: Location of La Reina site in Córdoba, Spain.

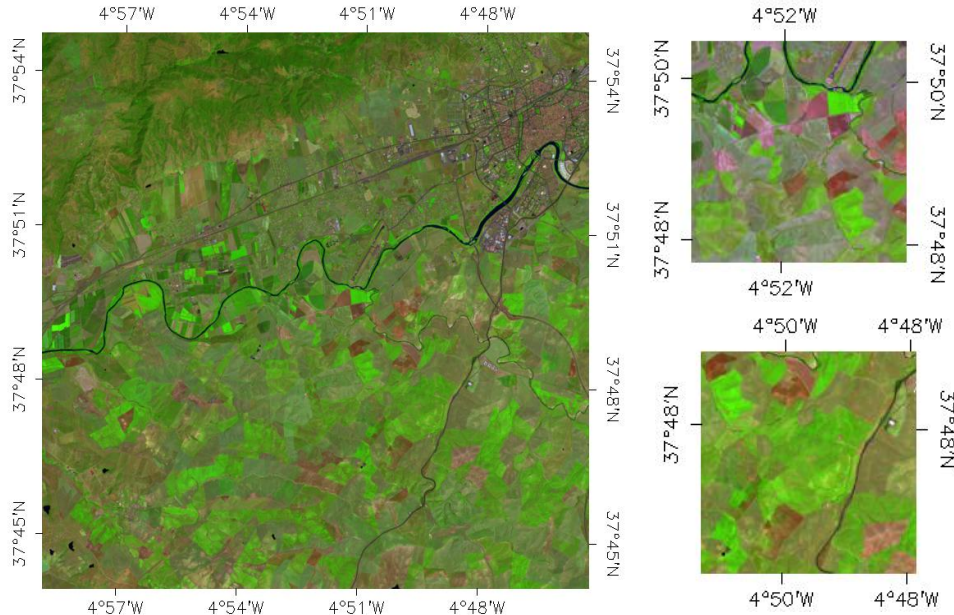


Figure 2: False color composition of TOA Reflectance Landsat-8 image over the $5 \times 5 \text{ km}^2$ study area (20th, May 2014) Left: $20 \times 20 \text{ km}^2$ image. Right: Subsite 1 (Top) and Subsite 2 (Bottom).

Table 1: Coordinates and altitude of the test site (centre).

La Reina - Cordoba	Site Center & subsite 1	subsite 2
Geographic Lat/lon, WGS-84 (degrees)	Latitude = 37.824086 N Longitude = 4.869247W	Latitude = 37.7929 N Longitude = 4.82668W
Altitude	120 m	120 m

3.2. DESCRIPTION OF THE TEST SITE

The study area is located in a depression of the valley of the Guadalquivir, close to the Córdoba city. The climate is Subtropical-Mediterranean, it has the highest summer average daily temperatures in Europe. Winters are mild with isolated frosts. Precipitation is concentrated in the coldest months; this is due to the Atlantic coastal influence. Precipitation is generated by storms from the west that occur most frequently from December through February. This Atlantic characteristic then gives way to a hot summer with significant drought more typical of Mediterranean climates. Annual rain surpasses 600 mm (24 in), although there is a recognized inter-annual irregularity.

The dominant vegetation for La Reina - Córdoba cropland is Wheat, Cotton, Onion, Sunflower, Potato, Olive tree plantation which is representative of the Region. Figure 3 is a description of the site, some images of these Landscapes are shown in Figure 4.

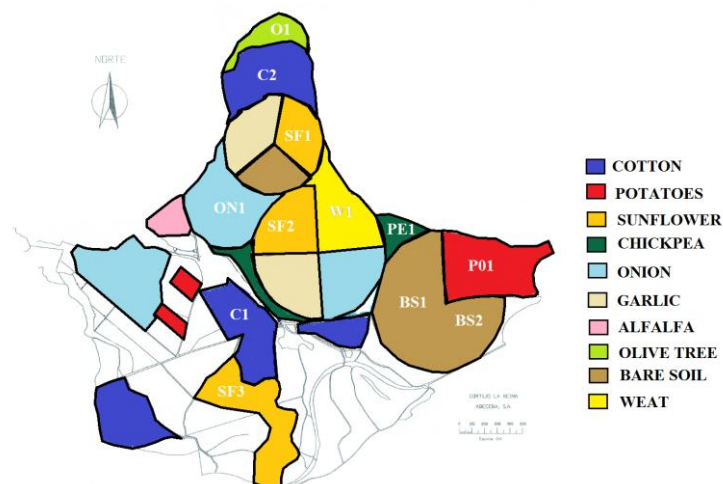


Figure 3: Distribution of the fields over the study area. La Reina site, Córdoba (Spain).

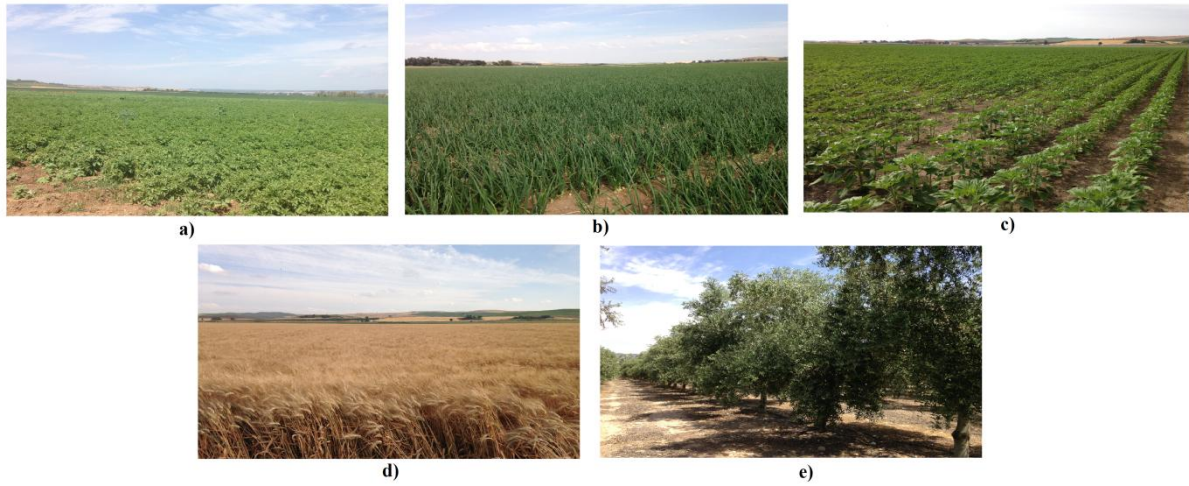


Figure 4: Examples of the different land cover types in La Reina site – Córdoba (Spain). a) Chickpea, b) Onion, c) Sunflower, d) Wheat and e) Olive Tree.

4. GROUND MEASUREMENTS

The ground measurement database reported here was acquired by EOLAB.

4.1. MATERIAL AND METHODS

Digital Hemispheric Photographs (DHP) were acquired with a digital camera. Hemispherical photos allow the calculation of LAI, FAPAR and FCOVER measuring gap fraction through an extreme wide-angle camera lens (i.e. 180°) (Weiss et al., 2004). It produces circular images that record the size, shape, and location of gaps, either looking upward from within a canopy or looking downward from above the canopy. The system is composed by a professional camera and a fisheye lens: CANON EOS 6D and a SIGMA 8mm F3.5 – EX DG.

Optical systems are not perfect it is needed to calibrate the system in order to determinate the Optical Centre and the Projection Function (Weiss, 2010). The optical centre is defined by the projection of the optical axis onto the CCD matrix where the image is recorded, for our dual system (camera and lens) was found in the point: (x=1378, y= 896) (Latorre et al. 2014).

The hemispherical photos acquired during the field campaign were processed with the CAN-EYE software (developed by INRA <http://www6.paca.inra.fr/can-eye>) to derive LAI, FAPAR and FCOVER. It is based on a RGB colour classification of the image to discriminate vegetation elements from background (i.e., gaps). This approach allows exploiting downward-looking photographs for short canopies (background = soil) as well as upward-looking photographs for tall canopies (background = sky). CAN-EYE software processes simultaneously up to 20 images acquired over the same ESU. Note that our images were acquired with similar illumination conditions to limit the variation of colour dynamics between images.

The processing is achieved in 3 main steps (Weiss et al., 2004). First, image pre-processing is performed, which includes removing undesired objects (e.g. operator, sun glint) and image contrast adjustments to ensure a better visual discrimination between vegetation elements and background. Second, an automatic classification (k-means clustering) is applied to reduce the total number of distinctive colours of the image to 324 which is sufficient to ensure accurate discrimination capacities while keeping a small enough number of colours to be easily manipulated. Finally, a default classification based on predefined colour segmentation is first proposed and then iteratively refined by the user. The allocation of the colours to each class (vegetation elements versus background) is the most critical phase that needs to be interactive because colours depend both on illumination conditions and on canopy elements. At the end of this process a binary image, background versus vegetation elements (including both green and non-green elements) is obtained.

The CAN-EYE software computes biophysical variables from gap fraction as follows:

Effective LAI (LAI_{eff}): Among the several methods described in Weiss et al (2004), the effective LAI estimation in the CAN-EYE software is performed by model inversion. The effective LAI is estimated from the Plant Area Index (PAI) which is the variable estimated by CAN-EYE, as no distinction between leaves or other plant elements are made from the gap fraction estimates. PAI is very close to the effective LAI for croplands when pictures are taken downward looking, whereas larger discrepancies are expected for forest when pictures are taken upward looking. Effective LAI is directly retrieved by inverting Eq. (1) (Poisson model) and assuming an ellipsoidal distribution of the leaf inclination using look-up-table (LUT) techniques.

$$P_0(\theta_v, \varphi_v) = e^{-N \cdot (\theta_v, \varphi_v)} = e^{-G \cdot (\theta_v, \varphi_v) \cdot \frac{LAI_{eff}}{\cos(\theta_v)}} \quad \text{Eq. (1)}$$

A large range of random combinations of LAI (between 0 and 10, step of 0.01) and ALA (Average Leaf Angle) (10° and 80° , step of 2°) values is used to build a database made of the corresponding gap fraction values (Eq.1) in the zenithal directions defined by the CAN-EYE user (60° for the DHP collection in this field campaign). The process consists then in selecting the LUT element in the database that is the closest to the measured P_0 . The distance (cost function C_k) of the k^{th} element of the LUT to the measured gap fraction is computed as the sum of two terms. The first term computes a weighted relative root mean square error between the measured gap fraction and the LUT one. The second term is the regularization term that imposes constraints to improve the PAI estimates. Two equations are proposed for the second “regularization” term:

(1) constraint used in CAN-EYE V5.1 on the retrieved ALA values that assume an average leaf angle close to $60^\circ \pm 03^\circ$, and

(2) constraint used in CAN-EYE V6.1 on the retrieved PAI value that must be close from the one retrieved from the zenithal ring at 57° . This constraint is more efficient, but it can be computed only when the 57° ring is available (i.e., $COI \geq 60^\circ$)

The software also proposed other ways of computing PAI and ALA effective using Miller’s formula (Miller, 1967) which assumed that gap fraction only depends from view zenith angle. Furthermore, the CAN-EYE makes an estimation using the Welles and Norman (1991) method used in LAI-2000 for 5 rings. These LAI2000-like estimates were not used here as are based on the same Miller’s formula but using limited angular sampling.

LAI: The actual LAI that can be measured only with a planimeter with however possible allometric relationships to reduce the sampling, is related to the effective leaf area index through:

$$LAI_{eff} = \lambda_0 \cdot LAI \quad \text{Eq. (2)}$$

where λ_0 is the clumping index. In CAN-EYE, the clumping index is computed using the Lang and Xiang (1986) logarithm gap fraction averaging method, although some uncertainties are associated to this method (Demarez et al., 2008). The principle is based on the assumption

that vegetation elements are locally assumed randomly distributed. Values of clumping index given by CAN_EYE are in certain cases correlated with the size of the cells used to divide photographs. The values reported here were estimated with an average of the three results (CEV6.1, CEV5.1 and Miller).

As the CAN-EYE software provides different results (CEV6.1, CEV5.1 and Miller's) for LAI and LAI_{eff} variables; an average LAI value was provided as ground estimate, and the standard deviation of the different method LAI estimates was reported as the uncertainty of the estimate (see associated 20140520_VGM_LaReina_Cordoba.xls file)

FCOVER is retrieved from gap fraction between 0 to 10°.

$$FCOVER = 1 - P_0 \cdot (0 - 10^\circ) \quad \text{Eq. (3)}$$

FAPAR: As there is little scattering by leaves in that particular spectral domain due to the strong absorbing features of the photosynthetic pigments, FAPAR is often assumed to be equal to FIPAR (Fraction of Intercepted Photosynthetically Active Radiation), and therefore to the gap fraction. The actual FAPAR is the sum of two terms, weighted by the diffuse fraction in the PAR domain: the 'black sky' FAPAR that corresponds to the direct component and the 'white sky' or the diffuse component.

The instantaneous "Black-sky FAPAR" ($FAPAR^{BS}$) is given at a solar position (date, hour and latitude). Depending on latitude, the CAN EYE software computes the solar zenith angle every solar hour during half the day (there is symmetry at 12:00). The instantaneous FAPAR is then approximated at each solar hour as the gap fraction in the corresponding solar zenith angle:

$$FAPAR^{BS}(\theta_S) = 1 - P_0 \cdot (\theta_S) \quad \text{Eq. (4)}$$

The daily integrated black sky or direct FAPAR is computed as the following:

$$FAPAR_{Day}^{BS} = \frac{\int_{sunset}^{sunrise} \cos(\theta_S) \cdot [1 - P_0 \cdot (\theta_S)] \cdot d\theta}{\int_{sunset}^{sunrise} \cos(\theta_S) \cdot d\theta} \quad \text{Eq. (5)}$$

The CAN-EYE software provides FAPAR Instantaneous and FAPAR daily integrated values as well. Only FAPAR instantaneous at 10:00 h SLT was up-scaled.

4.2. SPATIAL SAMPLING SCHEME

A total of 55 ESUs (Elementary Sample Unit) of 9 different land cover types were characterized during the campaign (see Table 2). A pseudo-regular sampling was used within each ESU of approximately 20x20 m². The centre of the ESU was geo-located using a GPS. The number of hemispherical photos per ESU ranges between 12 and 15.

Figure 5 shows the distribution of the sampling units over the experimental site. The ground measurements are spread across fields of Cotton, Asparagus, Sunflower, Onion, Wheat, Chickpea, Potato and tree plantation (Olive Tree). Ground dataset correspond to DHP images taken during the intensive field campaign.



Figure 5: Distribution of the sampling units (ESU) over the study area. DHP sampling and study zone of 5x5 km², over La Reina site, Córdoba (Spain).

Table 2 summarizes the number of sampling units (ESUs) per each crop type acquired during the field campaigns.

Table 2: Summary of the field measurements in La Reina site – Córdoba (Spain).

ESU internal code	Number of ESU's
	Field Campaign (20 th of May, 2014)
AS (Asparagus)	2
C (Cotton)	12
OT (Olive Tree)	3
SF (Sunflower)	15
ON (Onion)	5
W (Wheat)	5
CP (Checkpea)	5
P (Potato)	5
BS (Bare Soil)	3

4.3. GROUND DATA

4.3.1. Data processing

The software CAN-EYE version V6.1 was used to process the DHP images. Figure 6 shows some examples of DHP over several ESUs.



Figure 6: Digital Hemispherical Photographs acquired in La Reina site, Córdoba (Spain) during the intensive campaign of 19-20 May 2014.

As the methodology describes at 4.1, the LAI and effective LAI values were calculated with the average of different estimations (CEV6.1, CEV5.1 and Miller's). Figure 7 shows the inter-comparison between the three methods. For LAI_{eff}, the results are very similar, however for the LAI graph, the most faithful estimation is for CEV5.1.

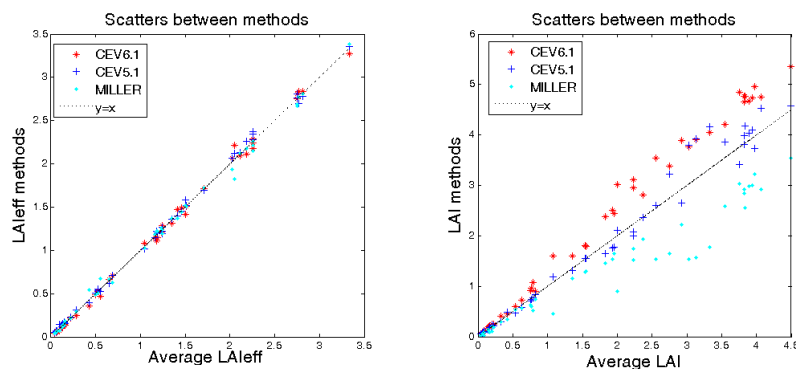


Figure 7: Intercomparison of the calculated biophysical variables LAI and LAI_{eff} over the ESUs with different methods: CEV5.1, CEV6.1 and Miller's formula. La Reina site – Córdoba (Spain) during the campaign of 20th May, 2014.

Figure 8 shows the intercomparison between LAI and Effective LAI with instantaneous FAPAR. For the FAPAR graphs the typical exponential positive exponential curve is evident, most clearly for LAI_{eff}.

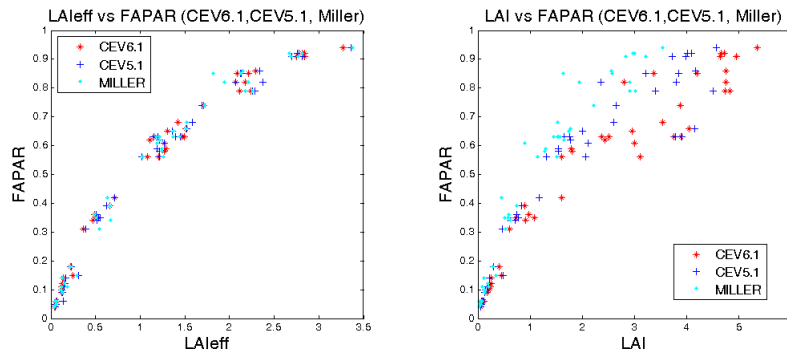


Figure 8: Intercomparison of the measured biophysical variables over the ESUs, Effective LAI and LAI versus FAPAR. La Reina site – Córdoba (Spain) during the campaign of 20th May, 2014.

Figure 9 shows the results of the CAN-EYE processing carried out on a cultivated area. (Onion). Different results of the CAN-EYE processing are selected: the masking, the classification of vegetation and the image generated by the software. Other graphs are shown: the average gap fraction and the clumping factor versus view zenith angle.

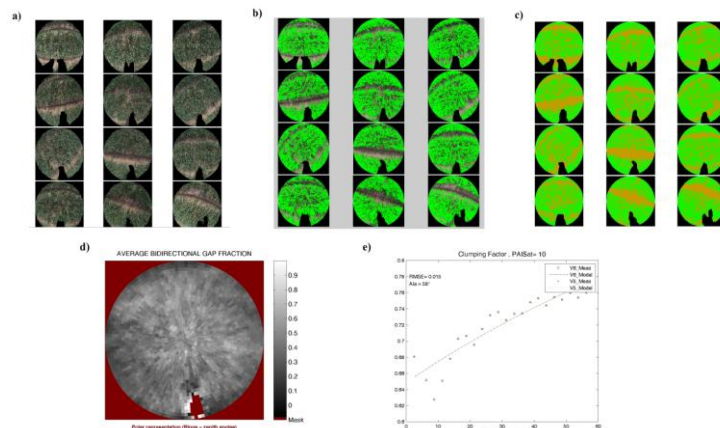


Figure 9: Results of the CAN-EYE processing carried out on cultivate area (ESU 19, Onion). (a) DHP images. (b, c) Classified images. (d) Average gap fraction and (e) the clumping factor versus view zenith angle.

4.3.2. Content of the Ground Dataset

Each ESU is described according to a standard format. The header of the database is shown in Table 3.

Table 3: The Header used to describe ESUs with the ground measurements.

Column	Var.Name	Comment
1	Plot #	Number of the field plot in the site
2	Plot Label	Label of the plot in the site
3	ESU #	Number of the Elementary Sampling Unit (ESU)
4	ESU Label	Label of the ESU in the campaign
5	Northing Coord.	Geographical coordinate: Latitude (°), WGS-84
6	Easting Coord.	Geographical coordinate: Longitude (°), WGS-84
7	Extent (m) of ESU (diameter)	Size of the ESU ⁽¹⁾
8	Land Cover	Detailed land cover
9	Start Date (dd/mm/yyyy)	Starting date of measurements
10	End Date (dd/mm/yyyy)	Ending date of measurements
11	Products*	Method
12		Nb. Replications
13		Products*
14		Uncertainty
		Instrument
		Number of Replications
		Methodology
		Standard deviation

*LAI_{eff}, LAI, FAPAR and FCOVER

Figures 10 to 13 show the measurements obtained during the field experiment. Figure 8 shows the LAI_{eff}, with values ranging from 0.1 (Cotton) to 3.2 (Potato). Similar distribution presents LAI, with higher values due to the clumping factor (Figure 11). Maximum values are for Potato and slightly lower for Cotton, that was in its early stages of growth. Other fields like Olive Tree Plantation, Chickpea and Sunflower (SF3) present values up to 3.

Figure 12 shows the FAPAR (daily integrated and instantaneous at 10:00 a.m.) values covering approximately the full dynamic range, with minimum values for cotton (0.04-0.18), medium to high absorption values for onion (around 0.5) and up to 0.9 for Potato. Slightly lower results were obtained for the instantaneous FAPAR at 10:00 h.

Figure 13 shows the FCOVER variable, quite similar to FAPAR.

Note that the values considered for Wheat were estimated with visual inspection due to the plants were at its last phenological phase completely dry, same for Bare Soils.

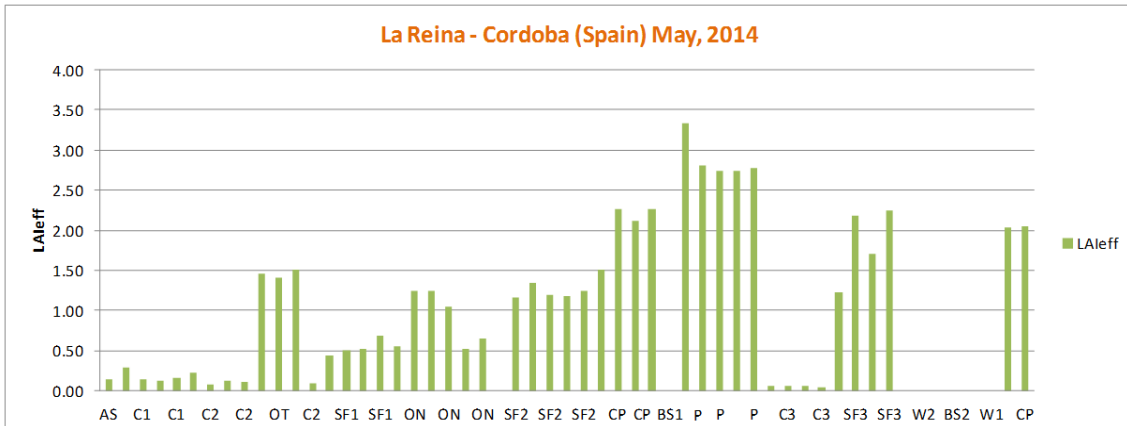


Figure 10: LAI_{eff} measurements acquired in La Reina site – Córdoba, during the campaign of May 2014. Distribution by ESUs. (AS: Asparagus, C: Cotton, OT: Olive Tree plantation, SF: Sunflower, ON: Onion, CP: Chickpea, P: Potato, W: Wheat and BS: Bare Soil)

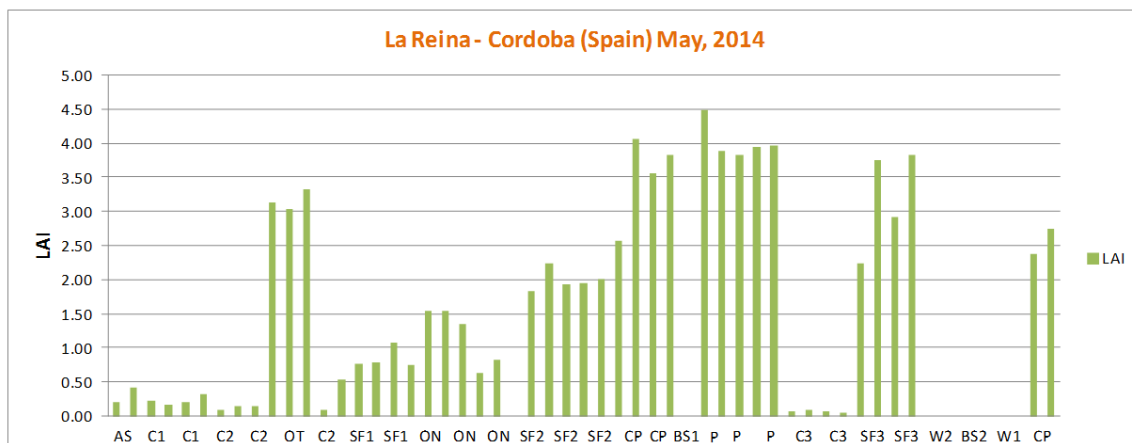


Figure 11: LAI measurements acquired in La Reina site – Córdoba, during the campaign of May 2014. As in figure 10 for LAI.

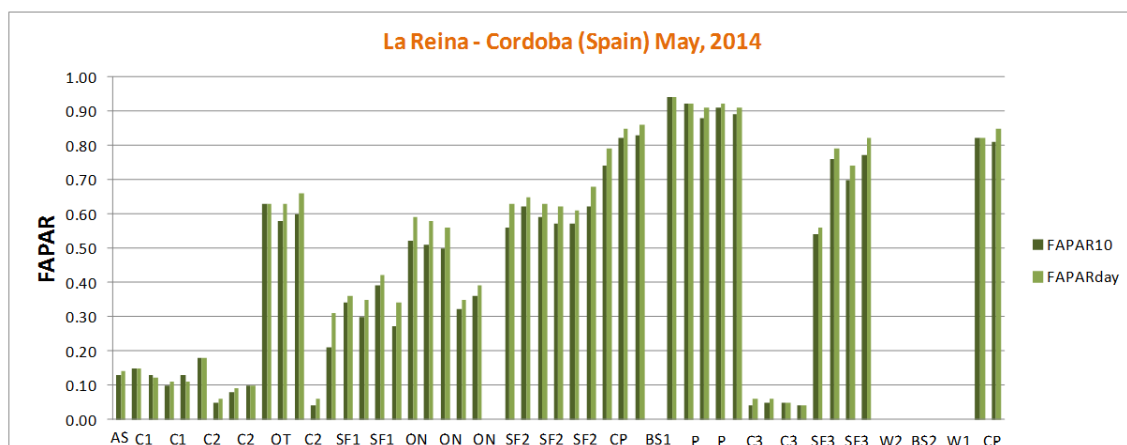


Figure 12: FAPAR instantaneous at 10:00h and FAPAR daily integrated measurements acquired in La Reina site – Córdoba, during the campaign of May 2014. As in figure 10 for FAPAR.

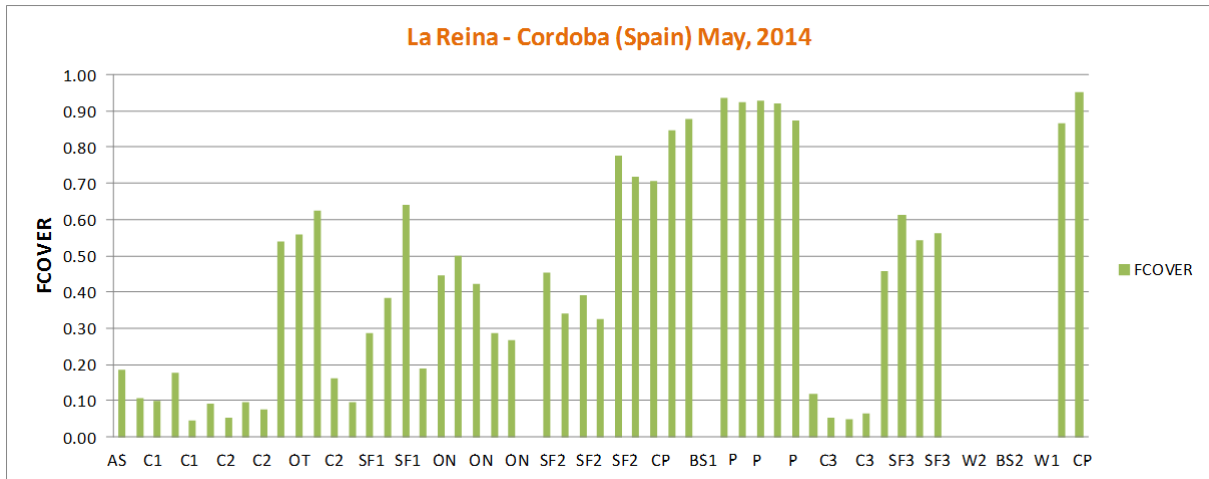


Figure 13: FCOVER measurements acquired in La Reina site – Córdoba, during the campaign of May 2014. As in figure 10 for FCOVER.

Figure 14 shows the distribution of the measured variables, covering the dynamic range of vegetation, with larger frequencies for lower values.

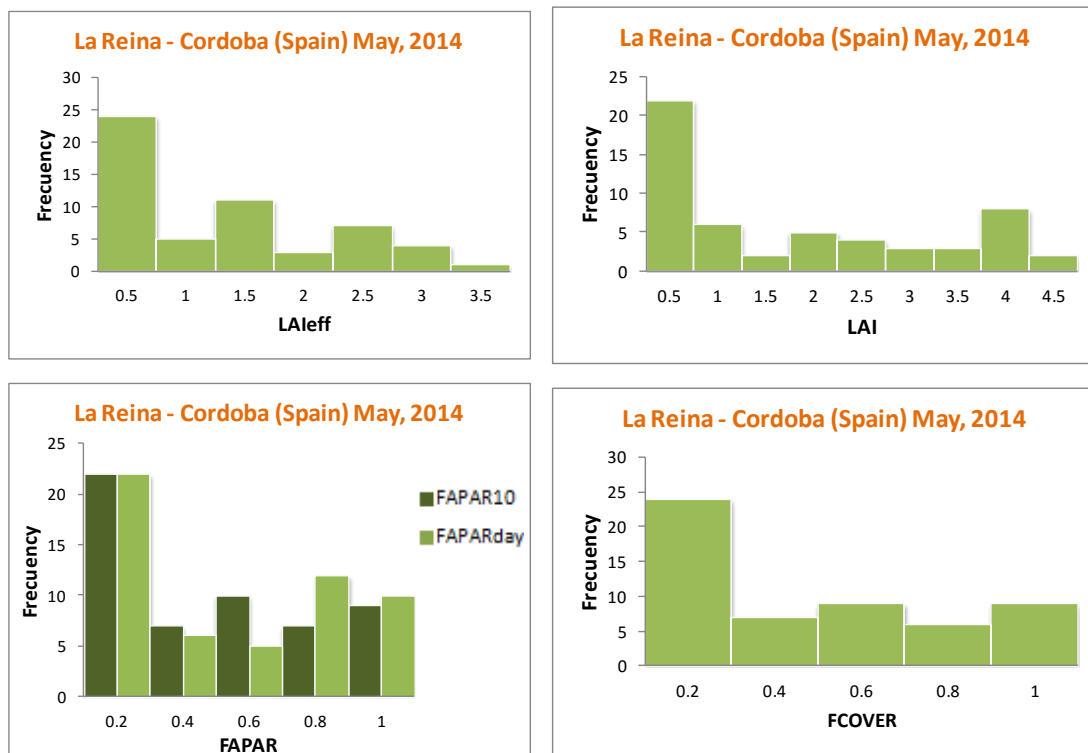


Figure 14: Distribution of the measured biophysical variables over the ESUs. La Reina site-Córdoba, during the campaign of 20th May, 2014.

5. EVALUATION OF THE SAMPLING

5.1. EVALUATION BASED ON CONVEX HULL: PRODUCT QUALITY FLAG.

The interpolation capabilities of the empirical transfer function used for up-scaling the ground data using decametric images is dependent of the sampling (Martinez et al., 2009). A test based on the convex hulls was also carried out to characterize the representativeness of ESUs and the reliability of the empirical transfer function using the different combinations of the selected bands (green, red, NIR and SWIR) of the Landsat-8 image. A flag image is computed over the reflectances. The result on convex-hulls can be interpreted as:

- pixels inside the 'strict convex-hull': a convex-hull is computed using all the Landsat-8 reflectances corresponding to the ESUs belonging to the class. These pixels are well represented by the ground sampling and therefore, when applying a transfer function the degree of confidence in the results will be quite high, since the transfer function will be used as an interpolator;
- pixels inside the 'large convex-hull': a convex-hull is computed using all the reflectance combinations ($\pm 5\%$ in relative value) corresponding to the ESUs. For these pixels, the degree of confidence in the obtained results will be quite good, since the transfer function is used as an extrapolator (but not far from interpolator);
- pixels outside the two convex-hulls: this means that for these pixels, the transfer function will behave as an extrapolator which makes the results less reliable. However, having a priori information on the site may help to evaluate the extrapolation capacities of the transfer function.

Figure 15 shows the results of the Convex-Hull test (i.e., Quality Flag image) for La Reina site over a $20 \times 20 \text{ km}^2$ area around the central coordinate site, and over the $5 \times 5 \text{ km}^2$ area provided. The strict and large convex-hulls are high around the test site for this zone, where the percentage evaluated there, it is 67 % for subsite 1 and 72% for subsite 2. Far away from the sampled area, at the left top corner of the image of $20 \times 20 \text{ km}^2$ size, there is an area corresponding to forest (*Sierra Morena* mountain range).

La Reina site – Córdoba 20th May, 2014

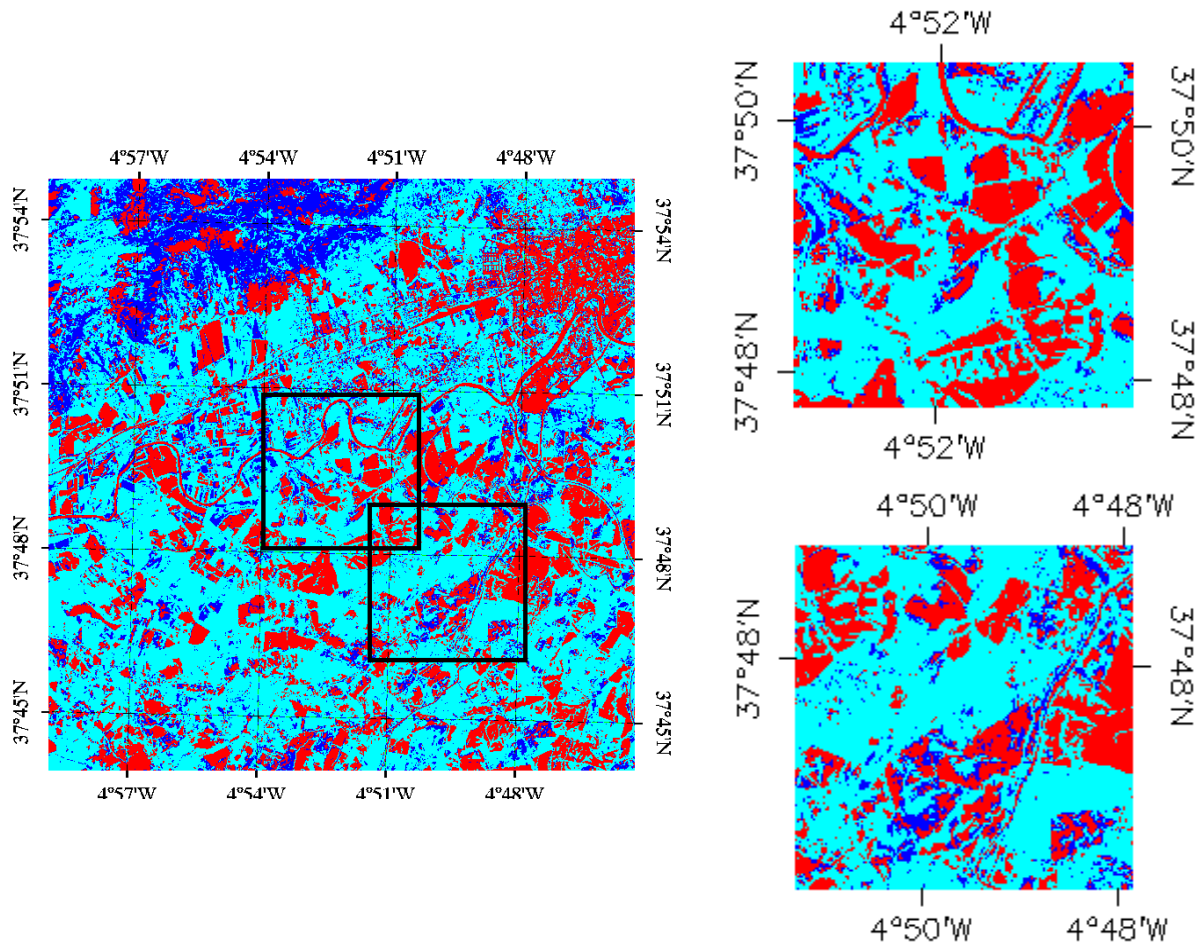


Figure 15: Convex Hull test over 20x20 km² (Left) extended area centered at the test site and the 5x5 km² study area (Right top: Subsite 1, Right bottom: Subsite 2). Clear and dark blue correspond to the pixels belonging to the 'strict' and 'large' convex hulls. Red corresponds to the pixels for which the transfer function is extrapolating, La Reina –Córdoba (20th May 2014).

6. PRODUCTION OF GROUND-BASED MAPS

6.1. IMAGERY

The Landsat-8 images were acquired the 17th May 2014 (see Table 4 for acquisition geometry). It corresponds to 4 spectral bands from 500 nm to 1750 nm with a nadir ground sampling distance of 30 m. For the transfer function analysis, the input satellite data used is Top of Atmosphere (TOA) reflectance. The original projection is UTM 30 North, WGS-84.

Table 4: Acquisition geometry of Landsat-8 data used for retrieving high resolution maps.

Landsat- 8 Metadata	
Platform / Instrument	Landsat- 8 / OLI_TIRS
Path	201
Row	34
Spectral Range	B3(green) : 0.53-0.59 μm B4(red) : 0.64-0.67 μm B5(NIR) : 0.85-0.88 μm B6(SWIR1) : 1.58-1.65 μm
May 2014 campaign	
Acquisition date	2014-05-17 10:55:54
Illumination Azimuth angle	130.606°
Illumination Elevation angle	65.102°
Ground Control Points Verify	121
Geometric RMSE Verify	4.487

6.2. THE TRANSFER FUNCTION

6.2.1. The regression method

If the number of ESUs is enough, multiple robust regression 'REG' between ESUs reflectance and the considered biophysical variable can be applied (Martínez et al., 2009): we used the 'robustfit' function from the Matlab statistics toolbox. It uses an iteratively re-weighted least squares algorithm, with the weights at each iteration computed by applying the bi-square function to the residuals from the previous iteration. This algorithm provides lower weight to ESUs that do not fit well.

The results are less sensitive to outliers in the data as compared with ordinary least squares regression. At the end of the processing, two errors are computed: weighted RMSE (using the weights attributed to each ESU) and cross-validation RMSE (leave-one-out method).

As the method has limited extrapolation capacities, a flag image (Figure 16), based on the convex hulls, is included in the final ground based map in order to inform the users on the reliability of the estimates.

6.2.2. Band combination

Figure 16 shows the errors (RW, RC) obtained for the several band combinations using TOA reflectance. Attending specifications of lower errors it has been chosen: band 1 (green), band 2 (red) band 3 (Near Infrared) and band 4 (Short Wave Infrared) combination of (1,2,3,4) = (G, R, N, S).

This combination on reflectance was selected for the transfer function since provides a good compromise between the low cross-validation RMSE, the weighted RMSE (lowest value) and the number of rejected points.

La Reina site – Córdoba 20th May, 2014

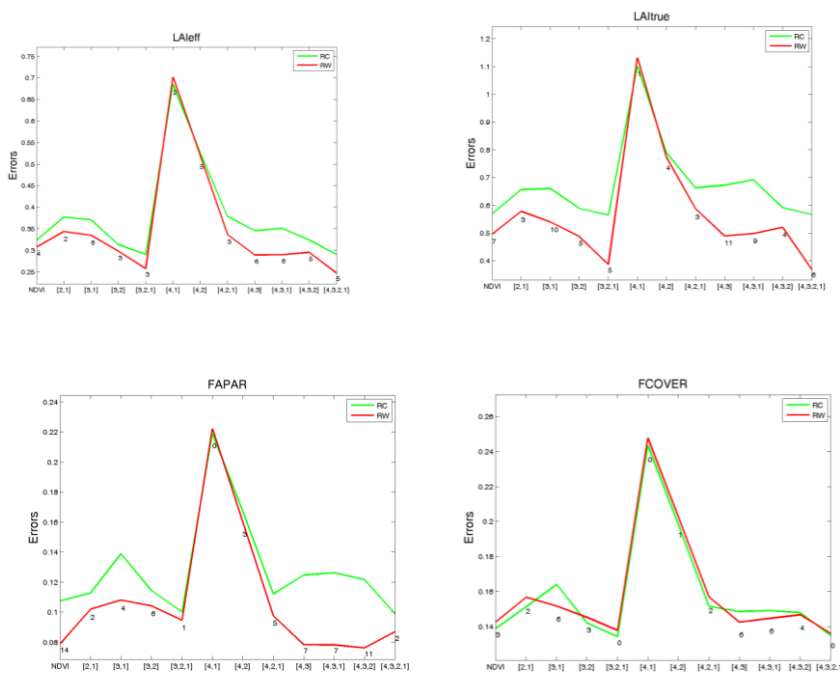


Figure 16: Test of multiple regression (TF) applied on different band combinations. Band combinations are given in abscissa (1=G, 2=RED, 3=NIR and 4=SWIR). The weighted root mean square error (RMSE) is presented in red along with the cross-validation RMSE in green. The numbers indicate the number of data used for the robust regression with a weight lower than 0.7 that could be considered as outliers.

6.2.3. The selected Transfer Function

The applied transfer function is detailed in Table 5, along with its weighted and cross validated errors.

Table 5: Transfer function applied to the whole site for LAleff, LAI, instantaneous FAPAR at 10:00 a.m. and FCOVER. RW for weighted RMSE, and RC for cross-validation RMSE.

Variable	Band Combination	RW	RC
LAleff	$-0.270962 - 0.000078 \cdot (\text{SWIR}) + 0.000075 \cdot (\text{NIR}) + 0.000465 \cdot (\text{R}) + 0.00055 \cdot (\text{G})$	0.247	0.281
LAI	$-0.661121 - 0.000058 \cdot (\text{SWIR}) + 0.000117 \cdot (\text{NIR}) - 0.00073 \cdot (\text{R}) + 0.000777 \cdot (\text{G})$	0.368	0.554
FAPAR 10:00	$0.006132 - 0.000033 \cdot (\text{SWIR}) - 0.000017 \cdot (\text{NIR}) - 0.000183 \cdot (\text{R}) + 0.000235 \cdot (\text{G})$	0.087	0.095
FCOVER	$-0.080759 - 0.0000227 \cdot (\text{SWIR}) + 0.000026 \cdot (\text{NIR}) - 0.000151 \cdot (\text{R}) + 0.000176 \cdot (\text{G})$	0.136	0.129

Figure 17 shows scatter-plots between ground observations and their corresponding transfer function (TF) estimates for the selected bands combinations. A good correlation is observed for the LAleff, LAI, FAPAR and FCOVER with points distributed along the 1:1 line and no bias, but showing some scattering mainly for FCOVER.

For FAPAR and FCOVER there are several dots over the TF axis, which corresponds to the senescent wheat cropland ESUS, where the empirical transfer function has a low overestimation in this type of cover.

La Reina site – Córdoba 20th May, 2014

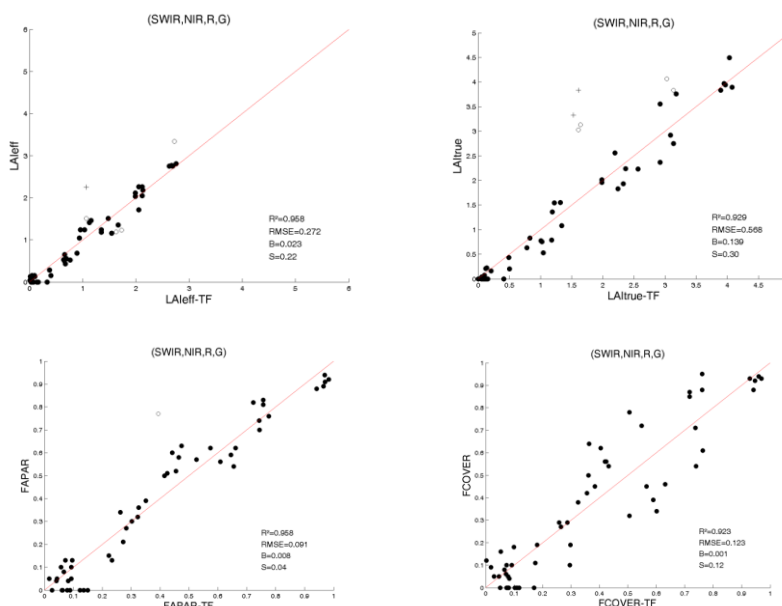


Figure 17: LAleff, LAI, FAPAR and FCOVER results for regression on reflectance using 4 bands combination. Full dots: Weight>0.7. Empty dots: 0<Weight<0.7 crosses.

6.3. THE HIGH RESOLUTION GROUND BASED MAPS

The high resolution maps are obtained applying the selected transfer function (Table 5) to the Landsat 8 TOA reflectance. Figures 18, 19 and 20 present the TF biophysical maps over the extended 20x20 km² area. Figure 15 shows the Quality Flag included in the final product.

La Reina site – Córdoba 20th May, 2014

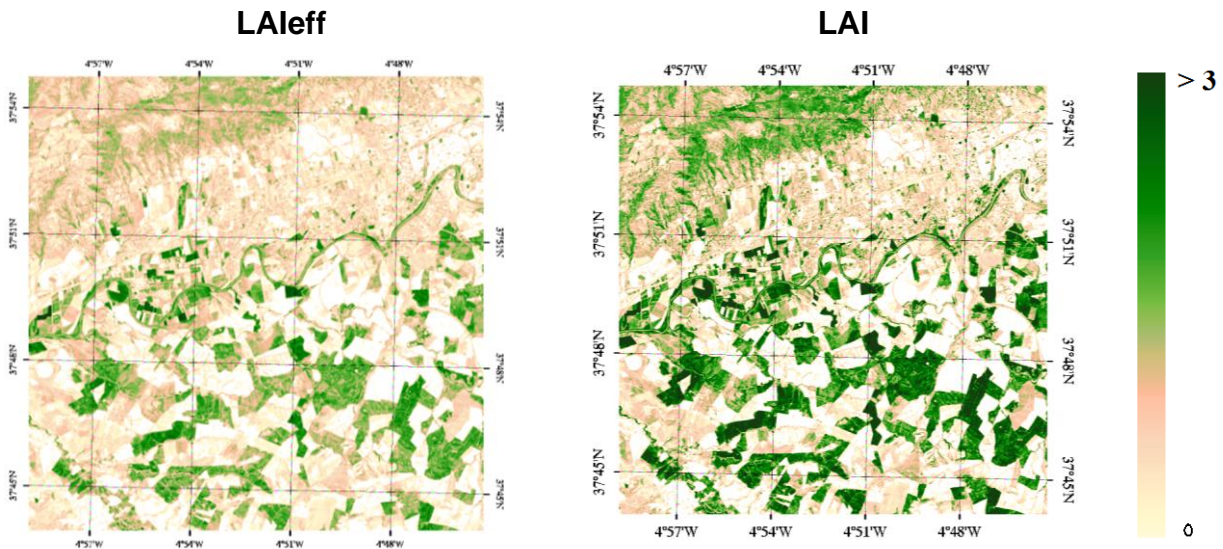


Figure 18: Ground-based LAI maps (20x20 km²) retrieved on the La Reina- Córdoba site (Spain). Left: LAIeff. Right: LAI. (20th May 2014).

La Reina site – Córdoba 20th May, 2014

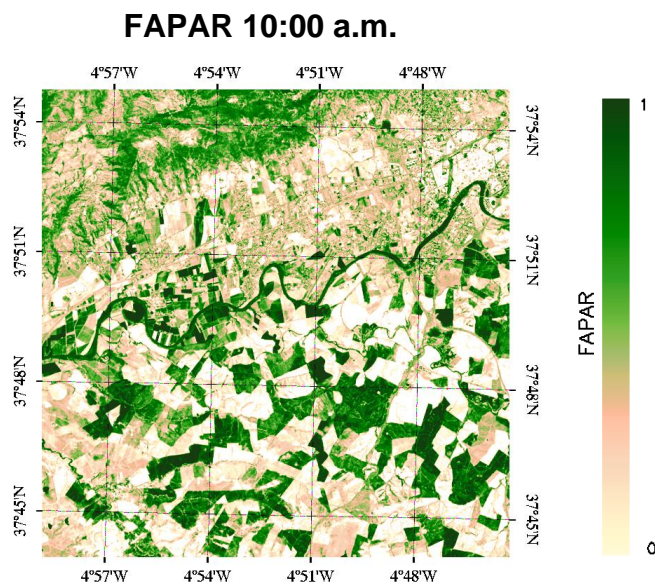


Figure 19: Ground-based FAPAR maps (20x20 km²) retrieved on the La Reina- Córdoba site (Spain). Top: Instantaneous FAPAR at 10:00 a.m. (20th May 2014).

La Reina site – Córdoba 20th May, 2014

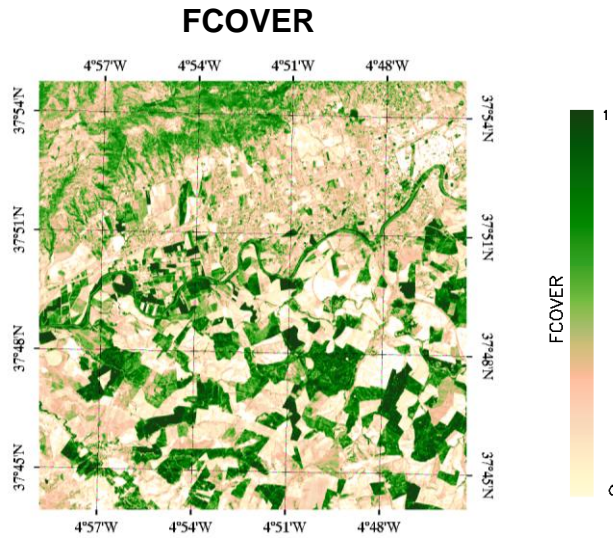


Figure 20: Ground-based FCOVER map (20x20 km²) retrieved on the La Reina- Córdoba site (Spain). (20th May 2014).

Figure 21 summarize these ground-based high resolution maps over the 5x5 km² study area. These maps are provided for validation of satellite products at different resolutions (see table 7).

La Reina site – Córdoba 20th May, 2014 – Subsite 1

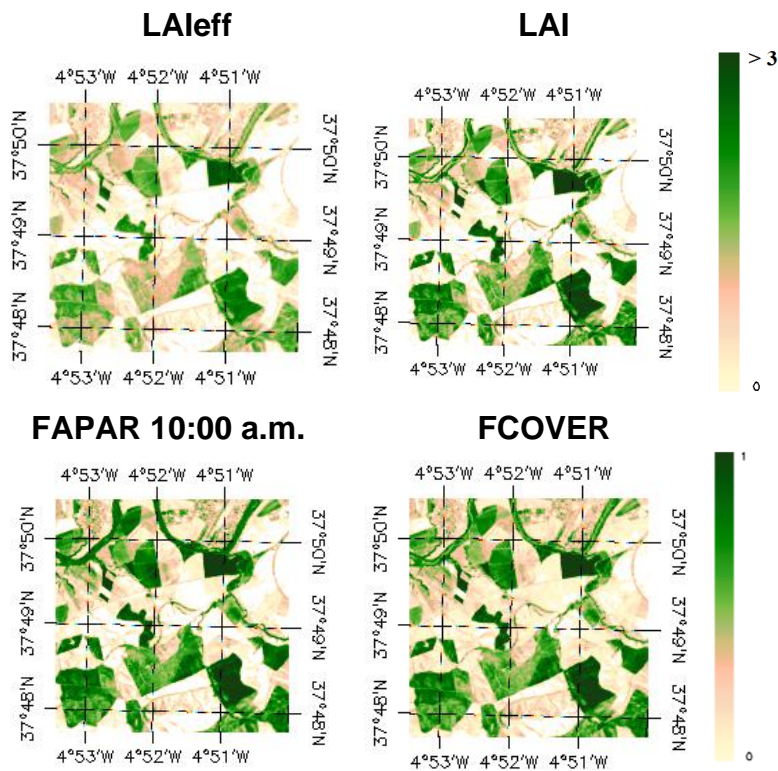


Figure 21: Ground-based maps (5x5 km²) retrieved on the La Reina- Córdoba site (Spain) subsite 1. (20th May 2014).

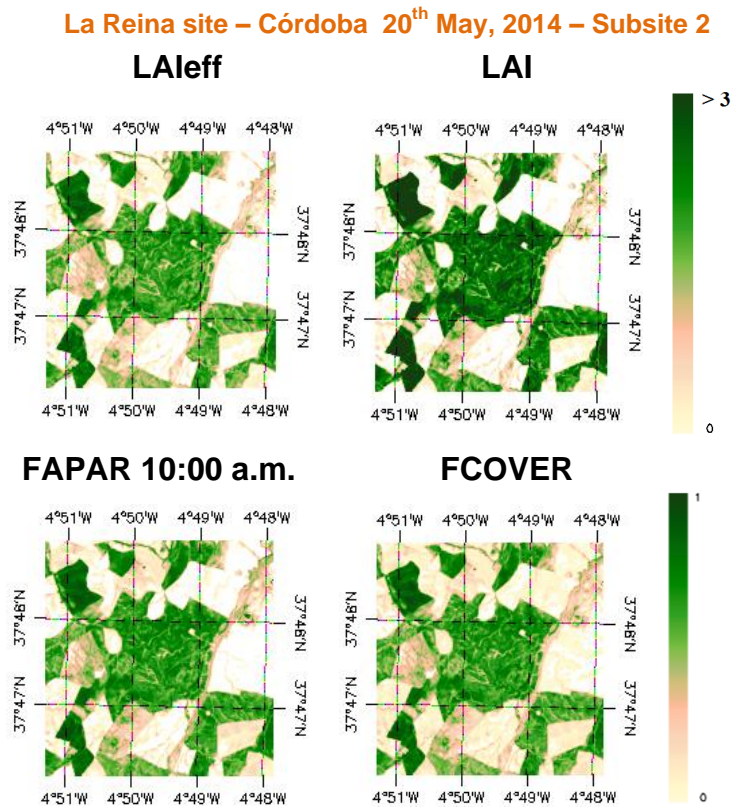


Figure 22: Ground-based maps (5x5 km²) retrieved on the La Reina- Córdoba site (Spain) subsite 2. (20th May 2014).

6.3.1. Mean Values

Mean values of a 3x3 km² area centred in the test site are provided for validation of 1 km satellite products in agreement with the CEOS OLIVE direct dataset (Table 6). For the validation of coarser resolutions product (e.g. MSG products) a larger area should be considered. For this reason, maps are provided at 5x5 km², and 20x20 km².

Table 6: Mean values and standard deviation (STD) of the HR biophysical maps for the selected 3 x 3 km² area at La Reina site – Córdoba (Spain).

		subsite 1		subsite 2	
		LATITUDE	LONGITUDE	LATITUDE	LONGITUDE
3x3 km ²		37.8189	-4.8624	37.7929	-4.82668
LAI _{eff}	MEAN	0.74		1.07	
	STD	0.78		0.68	
LAI	MEAN	1.08		1.59	
	STD	1.16		1.02	
FAPAR 10	MEAN	0.30		0.42	
	STD	0.28		0.25	
FAPAR day	MEAN	0.32		0.44	
	STD	0.30		0.26	
FCOVER	MEAN	0.30		0.41	
	STD	0.27		0.24	

Table 7: Content of the dataset.

Parameter	Dataset name	Range	Variable Type	Scale Factor	No Value
LAI effective	LAIeff	[0, 7]	Integer	1000	-1
LAI	LAI	[0, 7]	Integer	1000	-1
FAPAR 10:00 a.m.	FAPAR	[0, 1]	Integer	10000	-1
Fraction of Vegetation Cover	FCOVER	[0, 1]	Integer	10000	-1
Quality Flag	QFlag	0,1,2 (*)	Integer	N/A	-1

(*) 0 means extrapolated value (low confidence), 1 strict interpolator (best confidence), 2 large interpolator (medium confidence)

Table 7 describes the content of the geo-biophysical maps in the "BIO_YYYYMMDD_LANDSAT8_LAREINA_CORDOBA ETF_5x5" files.

Nomenclature: BIO_YYYYMMDD_SENSOR_Site_Subsite ETF_Area
 where:

BIO stands for Biophysical (LAIeff, LAI, FAPAR and FCOVER)

SENSOR = LANDSAT8

YYYYMMDD = Campaign date

Site = La Reina - Córdoba

Subsite = 1 and 2

ETF stands for Empirical Transfer Function

Area = window size 20x20 km² and 5x5 km²

7. CONCLUSIONS

The FP7 ImagineS project continues the innovation and development activities to support the operations of the Copernicus Global Land service. One of the ImagineS demonstration sites is located in a depression of the valley of the Guadalquivir river, close to the Córdoba city, in Andalusia (Spain), over a cultivated area on the bank of the river, La Reina.

This report first present the ground data collected during an intensive field campaign on 19th - 20th of May of 2014. The dataset includes 55 elementary sampling units where digital hemispherical photographs were taken and processed with the CAN-EYE software to provide LAI, LAI_{eff}, FAPAR and FCOVER values to characterize the natural vegetation of the area (cultivated) as well as an olive tree plantation plot in the study area.

Secondly, high resolution ground-based maps of the biophysical variables have been produced over the site. Ground-based maps have been derived using high resolution imagery (Landsat-8) according with the CEOS LPV recommendations for validation of low resolution satellite sensors. Transfer functions have been derived by multiple robust regressions between ESUs reflectance and the several biophysical variables. The spectral bands combination to minimize errors (weighted RMSE and cross-validation RMSE) were band 1 (green), band 2 (red) band 3 (Near Infrared) and band 4 (Short Wave Infrared) combination. The RMSE values for the several transfer function estimates are 0.27 for LAI_{eff}, 0.57 for LAI, 0.09 for instantaneous FAPAR at 10:00 hours, and finally 0.12 for FCOVER, with no bias.

The quality flag map based on the convex-hull analysis shows good quality over the 5x5 km² study areas: 67% and 72% of the area corresponds to the strict and large convex-hulls.

The biophysical variable maps are available in geographic (UTM 30 North projection WGS-84) coordinates at 30 m resolution over the 20x20 km² and 5x5 km² over the center site and an additional 5x5 km² subsite. Mean values and standard deviation for LAI_{eff}, LAI, FCOVER and FAPAR were computed over an area of 3x3 km² centered at the instrumented site.

8. ACKNOWLEDGEMENTS

This work is supported by the FP7 IMAGINES project under Grant Agreement N°311766. Landsat 8-HR images are provided through the USGS Global Visualization service. This work is done in collaboration with the consortium implementing the Global Component of the Copernicus Land Service.

Thanks to the *IFAPA* for the support and the organization of the Field Campaign, and the “La Reina” farm people for the facilities which allow us to characterize the site.

9. REFERENCES

- Baret, F. and Fernandes, R. (2012). Validation Concept. VALSE2-PR-014-INRA, 42 pp.
- Camacho, F., Cernicharo, J., Lacaze, R., Baret, F., and Weiss, M. (2013). GEOV1: LAI, FAPAR Essential Climate Variables and FCOVER global time series capitalizing over existing products. Part 2: Validation and intercomparison with reference products. *Remote Sensing of Environment*, 137: 310-329.
- Demarez, V., Duthoit, S., Baret, F., Weiss, M. and Dedieu, G. (2008). Estimation of leaf area and clumping indexes of crops with hemispherical photographs. *Agricultural and Forest Meteorology*. 148, 644-655.
- Fernandes, R., Plummer, S., Nightingale, J., et al. (2014). Global Leaf Area Index Product Validation Good Practices. CEOS Working Group on Calibration and Validation - Land Product Validation Sub-Group. *Version 2.0: Public version made available on LPV website*.
- Martínez, B., García-Haro, F. J., & Camacho, F. (2009). Derivation of high-resolution leaf area index maps in support of validation activities: Application to the cropland Barrax site. *Agricultural and Forest Meteorology*, 149, 130–145.
- Miller, J.B. (1967). A formula for average foliage density. *Aust. J. Bot.*, 15:141-144
- Morissette, J. T., Baret, F., Privette, J. L., Myneni, R. B., Nickeson, J. E., Garrigues, S., et al. (2006). Validation of global moderate-resolution LAI products: A framework proposed within the CEOS land product validation subgroup. *IEEE Transactions on Geoscience and Remote Sensing*, 44, 1804–1817.
- Latorre, C., Camacho, F., Pérez, Beget M.E. and Di Bella, C. (2014). "Vegetation Field Data and Production of Ground-Based Maps: 25 de Mayo site. La Pampa, ARGENTINA" report. 18 -20 (Available at ImagineS website: <http://fp7-imagines.eu/pages/documents.php>).
- Weiss, M., Baret, F., Smith, G.J., Jonckheere, I. and Coppin, P., (2004). Review of methods for in situ leaf area index (LAI) determination. Part II. Estimation of LAI, errors and sampling. *Agricultural and Forest Meteorology*. 121, 37–53.
- Weiss M. and Baret F. (2010). CAN-EYE V6.1 User Manual
- Welles, J.M. and Norman, J.M., 1991. Instrument for indirect measurement of canopy architecture. *Agronomy J.*, 83(5): 818-825.